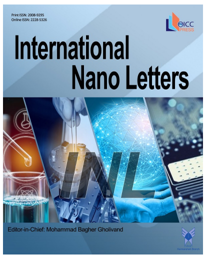

Volume 14, Issue 4, 142413 (1-9)

International Nano Letters (INL)

https://doi.org/10.57647/inl.2024.1404.13

Preparation of a New Inexpensive Paper-Based Sensor for the Detection of Nitrite and Nitrate Species in Water

Zahra Moradi[1], Parvaneh Ghaderi-Shekhi Abadi[1,3], Kambiz Varmira[4], Mohammad Joshaghani[1,2,*]

[1] *Institute of Nanoscience and Nanotechnology, Razi University, Kermanshah, Iran.*
[2] *Department of Inorganic Chemistry, Faculty of Chemistry, Razi University, Kermanshah, Iran.*
[3] *Department of Pharmaceutics, School of Pharmacy, Alborz University of Medical Sciences, Karaj, Iran.*
[4] *Department of Pharmaceutics, School of Pharmacy, Kermanshah University of Medical Sciences, Kermanshah, Iran.*

[*] **Corresponding author:** mjoshaghani@razi.ac.ir

Original Research

Abstract:

A low-cost, disposable, paper-based microfluidic analytical device (µPAD) has been developed for the measurement of nitrite and nitrate in water, with a color intensity-based response. The µPAD was fabricated using Whatman filter paper No. 1 and a glossy, self-adhesive backing. Nitrite was measured by the Griess reaction, and for nitrate determination, nitrate was reduced to nitrite in situ on the paper with zinc nanoparticles (ZnNPs). We chose ZnNPs because they outperformed zinc microparticles (ZnMPs). The system showed linear calibration ranges of 0.01 – 1.25 mM for nitrite and 0.04 – 1.25 mM for nitrate. The detection limits were 0.003 and 0.008 mM, respectively. The method showed no interference from common ions present in water. The results of real samples were consistent with the spectrophotometric reference method, so the proposed µPAD is suitable for rapid measurement of nitrite/nitrate concentrations at sampling sites of environmental and drinking waters.

Keywords:

Paper-based sensor; Colorimetric detection; Nitrite and nitrate species; Griess reaction; Zn nanoparticles

---

Cite this article: Moradi, Z., Ghaderi-Shekhi Abadi, P., Varmira, K., Joshaghani, M. Preparation of a New Inexpensive Paper-Based Sensor for the Detection of Nitrite and Nitrate Species in Water. *Int. Nano Lett.* **14**(4), 142413 (2024).

1. Introduction

Nitrate and nitrite are naturally occurring ions that are part of the nitrogen cycle [1, 2]. These ions are among the most important inorganic nitrogen species in drinking and environmental water resources. Besides In addition to being present in the natural nitrogen cycle, they also enter groundwater and surface water resources through the widespread use of nitrogen fertilizers in agriculture, the discharge of industrial wastewater, and urban sewage, and can lead to a decrease in dissolved oxygen and damage to aquatic ecosystems [3, 4]. From a human health perspective, when nitrite levels exceed the permissible limit (1.0 $\mathrm{mg{\cdot}N{\cdot}L^{-1}}$), it causes the blood not to carry enough oxygen by oxidizing hemoglobin to methemoglobin, especially in babies and pregnant women [5, 6]. Nitrite forms carcinogenic nitrosamines in the acidic conditions of the stomach [7, 8]. For this reason, recent studies have emphasized the need for continuous and sensitive monitoring of these species in environmental and biological samples [9]. Nitrate and nitrite concentrations can vary significantly depending on the region and time. Therefore, rapid and frequent detection of their concentrations, especially at the sampling site, can be crucial for timely water quality and risk management decisions. Conventional methods for nitrate and nitrite measurement include ion chromatography, high-performance liquid chromatography, capillary electrophoresis, spectrophotometric methods based on the Griess reaction, and a variety of electrochemical sensors. Although these methods are at a high level in terms of accuracy, sensitivity, and precision of results, they usually require expensive equipment, a well-equipped laboratory, relatively large sample and reagent volumes, a complex preparation process, and a trained operator, and are not practical options for large-scale field monitoring in deprived areas [10, 11]. Therefore, alongside these advanced laboratory methods, there is a need for simple, low-cost, multi-tasking, and portable systems for on-site nitrate/nitrite monitoring [12].

In the last two decades, microfluidic paper-based analytical devices (µPADs) have emerged as a promising platform for low-cost and portable analysis in the fields of medical diagnostics, food safety, and environmental monitoring [11, 13–16]. In these systems, fluid transfer and reactions are performed using the capillary properties of the paper, with no a pump or external power source, and the hydrophilic regions within the hydrophobic barriers on the paper allow for the definition of reactive and detection zone [17, 18]. µPADs are rapidly becoming a major platform for low-cost analytical instruments due to their extremely low fabrication cost, low sample and reagent consumption, compatibility with colorimetric, fluorimetric, and electrochemical detection methods, and their disposable nature. Innovative techniques in the fabrication and utilization of paper-based microfluidic detectors are rapidly expanding [18]. µPADs have effectively replaced costly laboratory tests with rapid on-site testing in the fields of food safety and environmental monitoring [19–21]. In a review, Yao et al. introduced paper-based sensors as a cost-effective, versatile, and accessible tool for the detection of a number of analytes [22]. The most important advantages of paper are mechanical properties, three-dimensional fibrous structure, biocompatibility and biodegradability, easiness of production and modification, reasonable price, and availability all over the world [19, 23].

In nitrate and nitrite determination, most reported colorimetric µPADs are designed based on the Griess reaction. In this reaction, nitrite reacts with sulfanilamide in an acidic medium and, after forming a diazonium ion, couples with N-(1-naphthyl)ethylenediamine to form a red azo dye, the intensity of which is proportional to the nitrite concentration [24]. For nitrate measurement, a reduction step to convert nitrate to nitrite is required. This step can be performed either off-site (e.g., in metal-containing reduction columns) or directly on paper. Despite the good performance of metal columns, environmental concerns, complexity of use, and the difficulty of integrating with paper substrates have motivated the development of on-site reduction methods [9, 25].

In recent years, several new µPADs have been reported for the measurement of nitrogenous species in water. Mako et al. built a sensor by implementing N-(1-Naphthyl) ethylenediamine-grafted cellulose on a paper-based device. They detected nitrite in a wide range of temperature, humidity, turbidity and salinity conditions [26]. The development of an analytical method involving a paper-based analytical device for the simultaneous determination of nitrite and sulfide colorimetry in water has been reported by Pereira et al. [27]. Badra et al. for the first to createa µPAD-based analytical device for the determination of nitrite and nitrate [28]. Tesfaye and Hussen developed a wax screen-printed µPAD for the simultaneous determination of nitrate and nitrite in water samples, in which the geometry of the channels and the Griess reaction conditions were optimized to achieve a suitable linear range and acceptable sensitivity [29]. In a study in 2022, a handheld hybrid polymer-paper platform was introduced that used Ionogel as a colorimetric medium for nitrite and a µPAD for in situ reduction and detection of nitrate, enabling simultaneous measurement of nitrate and nitrite in freshwater and saltwater [30]. Thongkam and Hemavibool developed an environmentally friendly, paper-based microfluidic analytical device for simultaneous colorimetric detection of nitrite and nitrate. Their system is low-cost and portable, suitable for field applications [31]. In 2021, Charbaji et al. developed a simple paper dip strip for colorimetric determination of nitrate and nitrite, which provides a user-friendly and inexpensive approach for environmental and food analysis [32]. Xie et al. used a novel method for fabrication paper-based devices by using a folded polydimethylsiloxane (PDMS)-coated paper mask [33]. Chiang et al. have fabricated Microfluidic paper-based analytical devices by 3D wax printing for glucose and nitrite Assays [34].

Despite these advances, significant challenges remain in the design of nitrate/nitrite-specific µPADs. In various designs, nitrate reduction to nitrite and the Griess reaction are performed in separate zones, sometimes on separate strips, requiring the user to perform multiple sequential steps, which complicates the task for non-specialists. Manufacturing approaches that use specialized patterning and printing steps or complex multi-part assemblies can increase cost and reduce accessibility for routine, large-scale work. Therefore, there remains a need for a low-cost, simple-to-manufacture, and easy-to-use paper-based system that integrates nitrate and nitrite concentration determination into a simple, single-step workflow while maintaining adequate analytical performance.

Here, we used a novel and cheaper technique for fabricating paper-based microfluidic devices by using Whatman filter paper (No. 1) and self-adhesive glossy paper for the detection of nitrite and nitrate ions in water. Nitrite was determined directly by using the Griess reaction, while nitrate was first reduced to nitrite. The reduction channel was covered with zinc particles, and the efficiency of zinc nanoparticles (ZnNPs) was compared with zinc microparticles (ZnMPs). This work particularly emphasizes the importance of a practical and easy-to-use design for on-site concentration determination, through (i) the use of readily available and inexpensive papers (Whatman No. 1 and self-adhesive glossy paper) to simplify the fabrication process and (ii) the integration of nitrate reduction on the paper for rapid measurement and general use. These features are of great interest for rapid monitoring of nitrate and nitrite in environmental and drinking water samples, especially where laboratory infrastructure is limited.

2. Materials and methods

2.1 Materials

$Zn(OAc)_2 \cdot 2H_2O$ ($\geq 99.9\%$, CN:5970-45-6), hydrazinium hydroxide (100%, CN:7803-57-8), and $NaH_2PO_4 \cdot 2H_2O$ ($\geq 98.0\%$, CN:13472-35-0) were purchased from Sigma-Aldrich, USA. Commercial ZnO (microparticle) was purchased from Pegah Roi Company. 1-Hexadecyltrimethylammonium bromide (CTAB, $\geq 98.0\%$, CN:57-09-0), Polyethylene glycol (PEG, M.W. = 1000 g/-mol, CN:25322-68-3), absolute ethanol (CN:64-17-5), sulfanilamide ($\geq 99.9\%$, CN:63-74-1), citric acid ($\geq 98.0\%$, CN:77-92-9), N-(1-naphthyl)ethylenediamine ($\geq 98.0\%$, CN:1465-25-4), sodium citrate tribasic hydrate ($\geq 99.0\%$, CN:6858-44-2), $NaNO_3$ ($\geq 99.9\%$, CN:7632-00-0), KNO_3

(≥ 99.0%, CN:7757-79-1), KCl (≥ 99.0%, CN:7447-40-7), NH_4Cl (≥ 99.5%, CN:12125-02-9), $NaNO_2$ (≥ 99.9%, CN:7632-00-0), and KNO_2 (≥ 99.0%, CN:7757-79-1) were purchased from Merck, Germany. Whatman filter paper No. 1 was purchased from Whatman international Ltd. Mudstone, England.

2.2 Methods and software

UV-Vis spectra were obtained with the Unico 2100 UV spectrophotometer, United Products & Instruments INC, USA. ZnNPs amount was determined by atomic absorption spectrometer (AAS) Perkin Elmer 1100-AAS model, United Kingdom, with a Zinc hollow cathode lamp. The size distribution and surface charge of compounds in ultrapure water were obtained using a dynamic light scattering (DLS), Malvern, UK laser analyzer, HPPS5001 model. The external morphology of compounds was measured by AIS 2100 microscope model with a resolution of 3.0 nm at 30 KeV, Seron Technologies INC, Korea. Scanning electron microscopy (SEM) samples were prepared by coating of solid particles with a conductive layer (gold). The images were obtained using a canon pixma mp160 scanner, Japan, with 300 DPI resolution and was processed by ImageJ software. The ultrasound irradiation for preparation of nano compounds was done by an Ultrasonic Homogenizer [400W-20kHz]-UP400-A model, TOP Sonics co, Iran.

2.3 Preparation of solutions

The stock solutions of NO_2^- and NO_3^- (10.0 mM) were prepared by dissolving 69.0 and 101.1 mg of sodium nitrite and potassium nitrate, respectively, in 100 mL water. The corresponding standard solutions were made from that. The Griess reagent was prepared by dissolving 50 mmol/L sulfanilamide, 330 mmol/L citric acid and 10 mmol/L N-(1-naphthyl)ethylenediamine [35]. The stock solution used in the interference studies, besides nitrate and nitrite, contained 20 mM of one of the following salts: $NaH_2PO_4 \cdot 2H_2O$, KCl, and NH_4Cl. ZnMPs suspension was prepared by pouring 500 mg of zinc powder into 10 mL of water [28]. ZnNPs was synthesized by the ultrasound method via a two-step method.

2.4 Preparation of ZnNPs

ZnNPs were prepared via a two-step method. Initially, nano zinc oxide was prepared by a typical synthesis [36, 37]. 2.5×10^{-2} mmol PEG (M.W. = 1000) and 2.7×10^{-2} mmol CTAB were dissolved in 4 mL ultrapure water (solution 1). In a separate beaker, 2 mmol $Zn(OAc)_2 \cdot 2H_2O$ was dissolved in 4 mL ultrapure water (solution 2). Solution 1 was then added dropwise to solution 2 under vigorous stirring. Then, hydrazinium hydroxide solution was added dropwise to the above solution to adjust the pH to 5-6. The resulting mixture was stirred to obtain a homogeneous solution. Finally, the solution was centrifuged, the obtained solid was added to 4 mL ultrapure water, and the suspension was ultrasonicated with 90 W power for 12 minutes. The resulting precipitate was collected, filtered and washed with ultrapure water and absolute ethanol several times and dried in vacuum. To prepare fresh ZnNPs, 2 mL of 10% w/w. PEG 1000 solution was added to 20 mL of 4000 ppm of the obtained nano zinc oxide under stirring for 30 minutes.

2.5 Design and fabrication of the paper-based device

Whatman filter paper No. 1 and a self-adhesive glossy paper were used. To prepare the device, the design was drawn with the CorelDraw Software and then the pattern was cut on the glossy paper by Cutting Plotter Graphtec (CE3000-60). The test site of µPAD comprised a detection zone (5 mm diameter), a transport channel (3 mm × 2 mm) and a reduction channel (13 mm × 4 mm). These zones were cut on Whatman filter paper No. 1 and clutched in the center of self-adhesive glossy paper (Fig. 1). The reduction channel was covered with 25 µL of the appropriate reducing agent, and the detection zone was wetted with 1-2 µL of the Griess reagent. The paper was dried in an oven at 60 °C for 10 min. After the reduction at the reduction zone, the resulting nitrite then could achieve to the test zone, react with the Griess reagent and produce a colored surface.

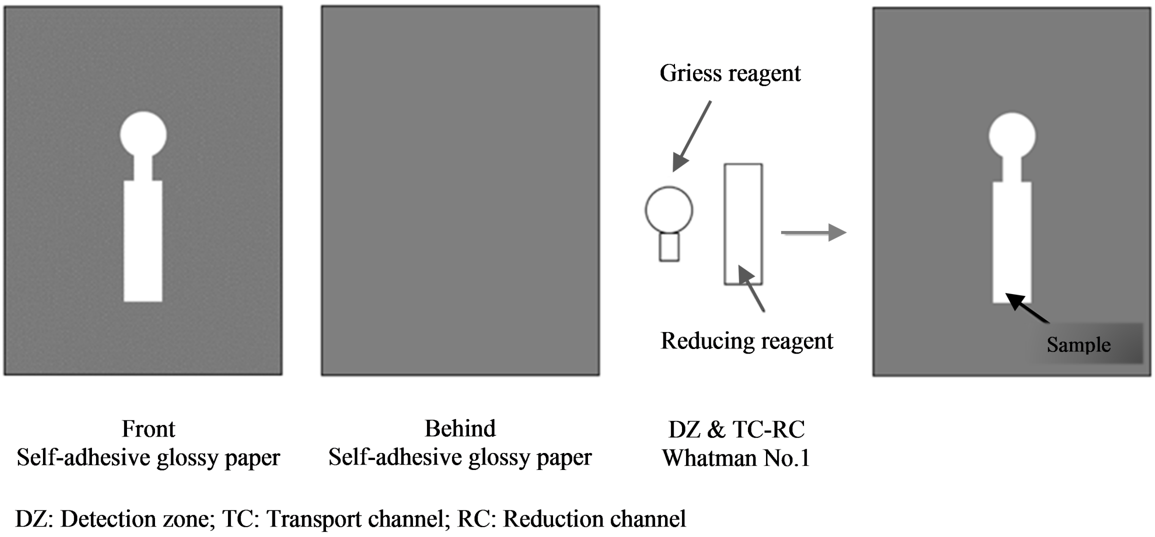

Figure 1. Schematic of the paper-based sensor.

2.6 Analytical procedure

Aqueous standard samples of nitrite and nitrate ions were deposited on the µPADs. The capillary driving force conducted the samples into the detection zone, and a red-violet color was developed because of thereaction of nitrite and the Griess reagent at ambient temperature (20-25 °C). After 5 minutes, the detection zone was scanned by a flatbed scanner, and the image was processed by the ImageJ software. The data obtained from the color intensity was transferred to Microsoft Excel. The plot of color intensity based on color indices as a function of concentration resulted in a linear calibration equation. The concentration of nitrite and nitrate ions in four real samples (obtained from well water and Poultry wastewater) was determined using the proposed µPAD method.

The interference of common ions such as K^+, Na^+, Cl^-, PO_4^{3-} and NH_4^+ was studied by analyzing standard solutions containing nitrite and nitrate in the presence of 20 mM of one of these ions.

The stability of µPADs was studied by performing daily tests for approximately 10 days on µPADs stored under two different conditions. Group A was µPADs stored at the ambient temperature after being prepared and covered with a laminate layer in a dark place, while group B was those stored in the refrigerator.

3. Results and discussion

Determination of nitrite ion concentration was performed directly based on the Griess reaction (Fig. 2), which involves a diazo-coupling procedure. The main principle of this method is that under acidic conditions, nitrite reacts with sulfanilamide to form a diazonium cation which subsequently couples to the aromatic amine N-(1-naphthyl)ethylenediamine (NED) to produce a red-violet colored ($\lambda_{max} \approx 540$ nm), water-soluble azo dye [37].

3.1 Data processing

Nitrite ions were detected directly by the Griess method. The concentration of nitrate was determined colorimetry from the difference in color intensity of the corresponding experiments with and without the reductant. Standard samples with specified concentrations were deposited on the bottom of µPADs (with/without the reducing agent).

3.2 Application of ZnNPs and ZnMPs as reducing agents

Given that Badra et al. used ZnMPs to reduce nitrate to nitrite [28], we used ZnMPs and ZnNPs for the same purpose. The obtained ZnNPs were sufficiently active to reduce nitrate to nitrite. The morphology of the nanoparticles surface has been investigated using SEM. Figure 3 shows that the produced particles are uniform and are nano-sized. The DLS analysis showed that the size of the produced nanoparticles was 73 nm and the surface charge was + 26 mV.

Deposition of ZnMPs on the paper was more difficult than ZnNPs. In addition, microparticles were not uniformly covering the paper (Fig. 4). The color intensity of the paper contains micro particles was also less than nanoparticles (Fig. 4). Therefore, ZnNPs was chosenfor further investigation.

To investigate the side effects of ZnNPs on the determination of nitrite, standard solutions of nitrite ions were prepared and tested under optimum experimental conditions in the presence and absence of ZnNPs. The results showed that the intensity of the color was the same in both cases. The presence of a reducing agent did not interrupt on nitrite determination.

3.3 Analytical procedure and plotting calibration curves

Two individual series of six experiments involving different concentration of nitrite and nitrate ions were used to investigate the applicability of the µPADs and plotting the calibration curves (Table 1).

The µPADs employed in the first series were free of reducing agent, while in the second series an appropriate amount of the reducing agent was deposited onto the reducing channel. Nitrate could be reduced to nitrite in the presence of a reducing agent and therefore, the obtained color in series two, is more intense. From the results of the first series, the concentration of nitrite could be determined, and from the second series, total concentration of nitrite and nitrate (reduced to nitrite) could be determined (Fig. 5).

The color intensity in the first series of experiments was employed for direct determination of nitrite concentration. The difference in color intensity between two mutual series was considered as a measure of nitrate ion concentration. The linear calibration diagrams and their equations for nitrite and nitrate have been shown in (Fig. 6) and (Fig. 7),

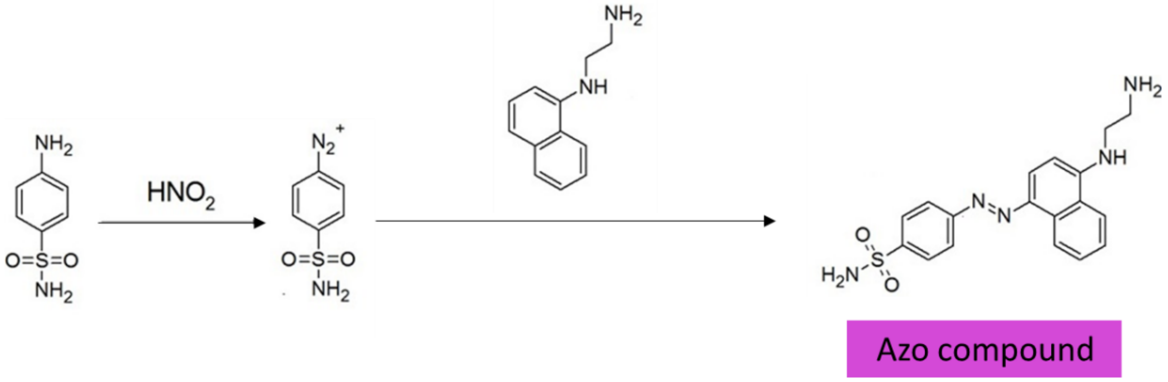

Figure 2. The Griess assay.

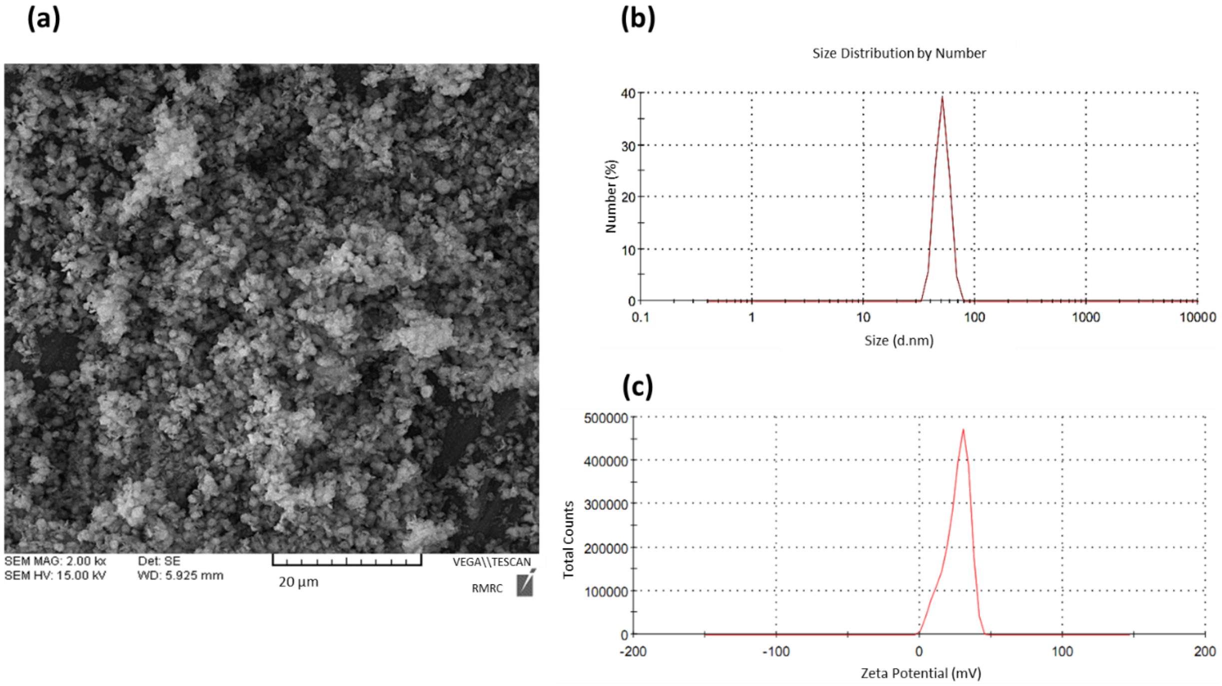

Figure 3. (a) SEM images, (b) particle size, and (c) zeta potential of the ZnNPs.

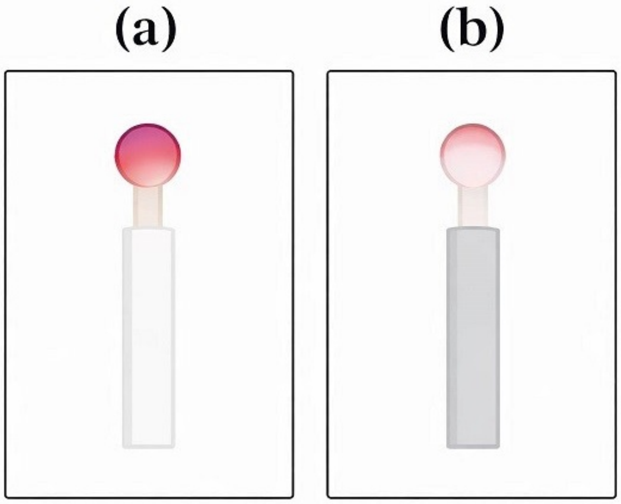

Figure 4. The color intensity due to reduction of nitrate to nitrite in the presence of (a) ZnNPs and (b) ZnMPs.

respectively. Under optimum conditions, the linear calibration ranges of the paper-based method for nitrite and nitrate are 0.01 – 1.25 and 0.04 – 1.25 respectively.

Under optimum conditions, the proposed paper-based was characterized by linear Calibration ranges for nitrite and nitrate of 0.01 – 1.25 and 0.04 – 1.25 mM, respectively, and the calibration equation was $\mathrm{GSV(nitrite)} = 2010.8 \times \mathrm{C}_{\mathrm{Nitrite}} + 419.76$ ($\mathrm{R}^2 = 0.9986$) and $\mathrm{GSV(nitrate\ and\ nitrite)} - \mathrm{GSV(nitrite)} = 683.65 \times \mathrm{C}_{\mathrm{Nitrate}} + 306.81$ ($\mathrm{R}^2 = 0.9816$), respectively. The limit of blank (LOB), the limit of detection (LOD) and the limit of quantification (LOQ) be calculated based on the standard deviation of blank and the slope of the calibration curve according to the following equations:

$$\mathrm{LOB} = \frac{\mathrm{SD}}{\mathrm{Slope}} \times 1.65 \tag{1}$$

$$\mathrm{LOD} = \frac{\mathrm{SD}}{\mathrm{Slope}} \times 3.33 \tag{2}$$

$$\mathrm{LOQ} = \frac{\mathrm{SD}}{\mathrm{Slope}} \times 10 \tag{3}$$

Table 1. Griess reagent volume, zinc colloidal nanoparticles volume, volume and concentration of standard solutions containing nitrite and nitrate on each of the µPADs.

µPADs	Griess reagent (µL)	ZnNPs (µL)	Standard volume (µL)	Nitrite (mM)	Nitrate (mM)
1	2.0	25.0	17.0	1.25	1.25
2	2.0	25.0	17.0	0.63	0.63
3	2.0	25.0	17.0	0.31	0.31
4	2.0	25.0	17.0	0.16	0.16
5	2.0	25.0	17.0	0.08	0.08
6	2.0	25.0	17.0	0.04	0.04

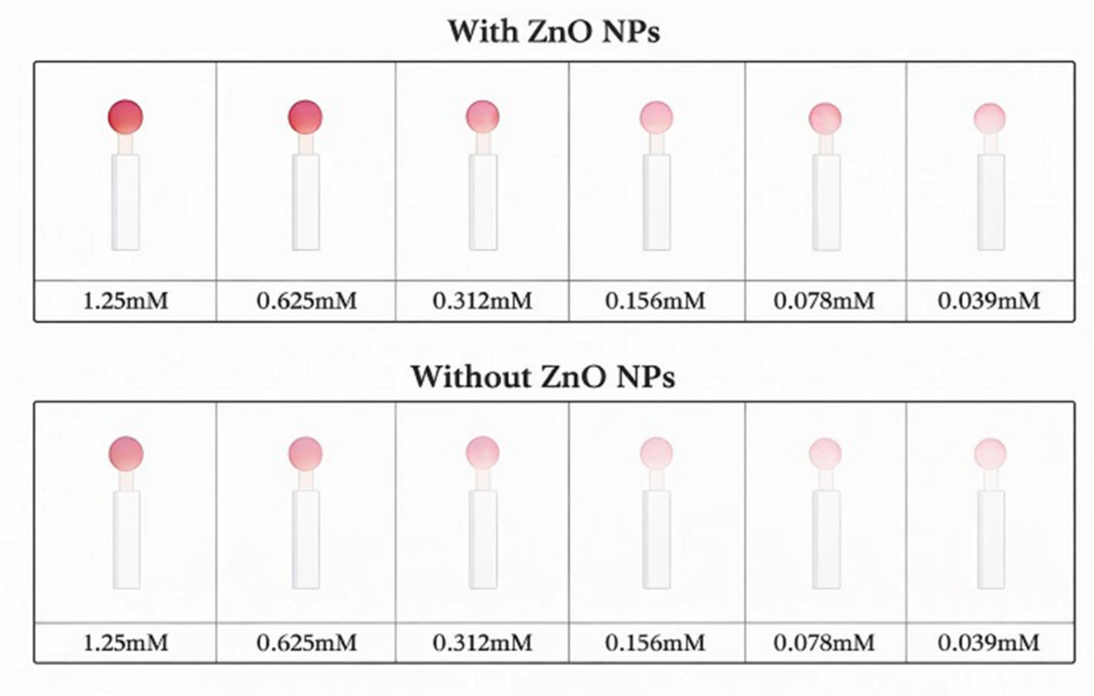

Figure 5. Images resulting from various concentrations of nitrate and nitrite (1.25, 0.63, 0.31, 0.16, 0.08, and 0.04 mM) at presence and absence ZnNPs.

SD of blank was 1.657. So, the LOB, LOD and LOQ for nitrite were 0.001, 0.003 and 0.008 mM, respectively. The corresponding LOB, LOD and LOQ for nitrate were 0.004, 0.008 and 0.024 mM, respectively.

Careful investigation of experimental details showed us that the time lag between appearing the color and scanning the image has a dominant effect on the color intensity. To investigate this effect, different time lags were investigated. The results showed that the best performance is obtained when the time lag is approximately 5 minutes (Fig. 8). The color intensity does not perfectly appear at time lags less than 5 minutes, while at time lags greater than 10, the intensity of the color is decreased progressively, which may be due to destruction of the azo dye compound.

3.4 The effect of interfering with other ions

We did new experiments using standard solutions containing 0.5 mM nitrite and 0.5 mM nitrate in the presence of the most important ions present in drinking and ground water to investigate the possible interference with nitrite/nitrate determination. The supplier's salts have also beenselected in a manner to cover an accountable range of water pH. Overall, neutral KCl, weak base NaH_2PO_4, and weak acid NH_4Cl were selected. The color intensity remained intact in the presence of these salts, which means these ions do not interfere with nitrate/nitrite determination.

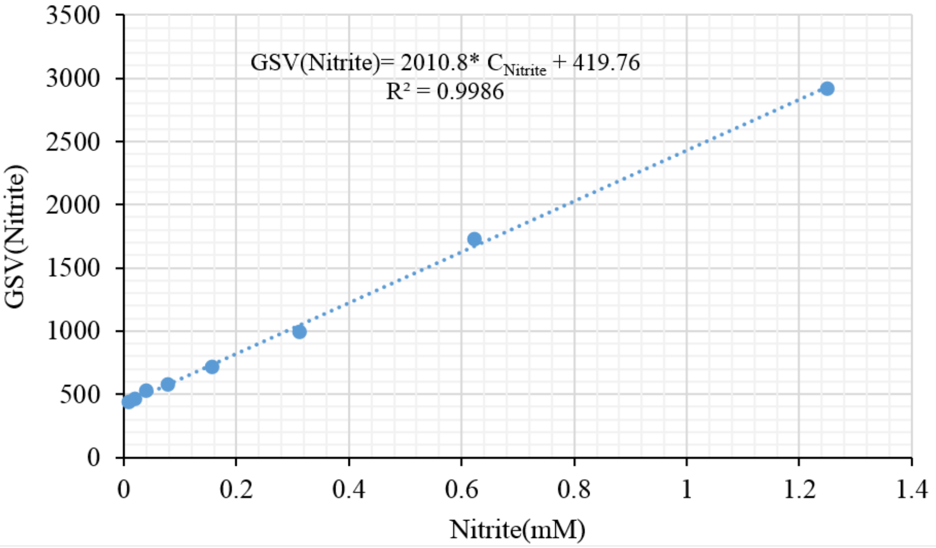

Figure 6. The calibration curve for nitrite; The GSVs as a function of the concentration of nitrite ion. The linear zone between 0.01 – 1.25 mM was selected.

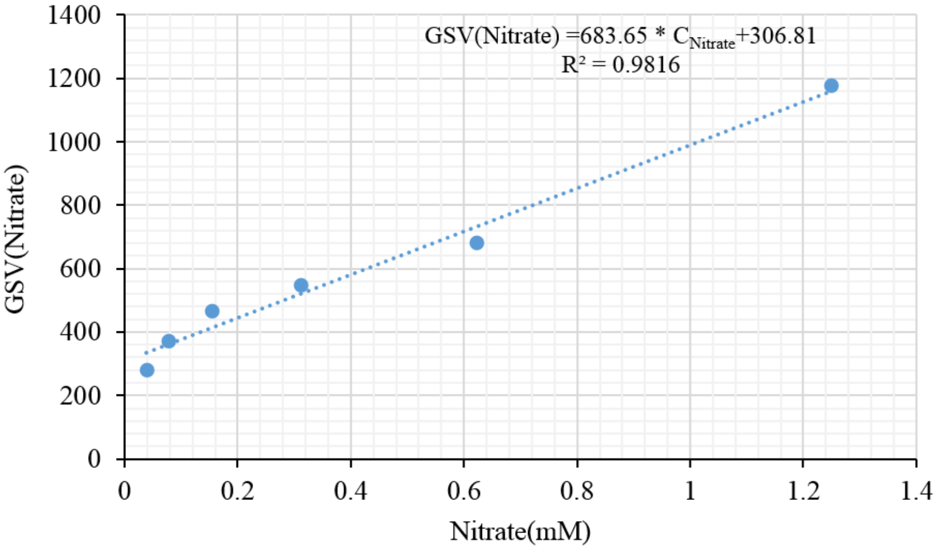

Figure 7. The calibration curve for nitrate; The GSVs as a function of the concentration of nitrate ion. The linear zone between 0.04 – 1.25 mM was selected.

3.5 Analysis of real samples

The concentrations of nitrite and nitrate in four real samples were determined using the proposed µPADs, and the results were compared with those obtained spectrophotometrically as a standard method. The results have been summarized in Table 2 and show very excellent agreement between two methods and reveal we can use the µPADs method as an alternative method of nitrate and nitrite determination. The F-test two Sample statistical analysis was also performed for variances. These methods yield the same results, with 95% confidence.

3.6 Lifetime and stability of µPADs

The lifetime of µPADs was studied by performing daily tests for approximately 10 days in two different conditions. Group A µPADs were covered with a laminate layer after being prepared and stored at ambient temperature in a dark place, while group B were stored in the refrigerator. The results showed that group a µPADs responded accurately for up to 2 days, but from the third day, a significant decrease in color intensity was observed. A similar decrease in intensity was observed for group B µPADs after 6 days. In this study, the linear response range was 0.01 – 1.25 mM for nitrite and 0.04 – 1.25 mM for nitrate. Also, the LOD for nitrite and nitrate was determined to be 0.003 and 0.008 mM, respectively. The results indicate the sensitivity and analytical performance of the µPAD designed for the simultaneous measurement of these two anions in aqueous samples. In comparison with previous studies, Francisca et al. in 2020 reported a linear range of 5 to 250 µM for nitrite and 0.2 to 1.2 mM for nitrate using a paper-based method, and obtained LOD of 0.005 µM and 0.08 mM for nitrite and nitrate, respectively [24]. The µPADs in another study could measure nitrite at 10 – 150 µM and nitrate at

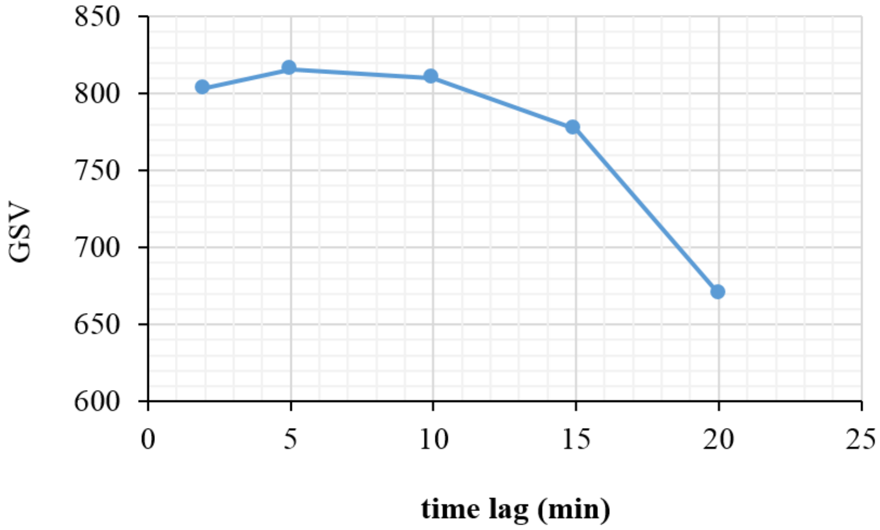

Figure 8. The effect of time lag on the color. Standard solutions of NO_2^- and NO_3^- with the concentrations 0.04 mM, from both ions. The volume of Griess reagent, standard samples and ZnNPs (200 ppm) were 2.0 µL, 17.0 µL and 25.0 µL, respectively.

Table 2. Analysis of nitrite and nitrate in real samples by µPADs and spectrophotometry.

Real samples	Nitrite(mM)		Nitrate(mM)	
	Spectrophotometry (mM)	µPAD (mM)	Spectrophotometry (mM)	µPAD (mM)
Sample 1	0.070	0.069	0.278	0.272
Sample 2	0.111	0.110	0.661	0.655
Sample 3	0.063	0.065	0.388	0.376
Sample 4	0.034	0.034	0.173	0.180

50 – 1000 µM [28]. Also, in a microfluidic paper-based analytical device fabricated by wax screen printing, a relatively narrow linear range was reported for nitrite (0.4 – 2.0 mg/L) and the LODs for nitrite and nitrate were 0.16 and 0.87 ppm, respectively [29]. In another study, in which vanadium (III) chloride was used as the reducing agent for nitrate to nitrite, the LOD for nitrate was 3 ppm and the LOD for nitrite was 0.522 ppm [32]. Comparison of the results shows that the use of vanadium (III) chloride not only requires a longer reduction time but also shows poorer performance in terms of accuracy and efficiency than the use of zinc particles [32]. In most previous studies, zinc powder or micronized particles have been used for nitrate reduction [24, 28], while in the present study, zinc nanoparticles (ZnNPs) were used for the first time as a reducing agent, which showed better performance than micronized particles. In terms of selectivity, the µPAD designed in this study, similar to some previous reports [28, 29], did not show any interference from common ions present in water. This indicates the high efficiency of the µPAD in detecting nitrite and nitrate ions based on the Griess reaction, without being affected by other environmental ions. As mentioned, the stability of µPADs was also studied. The results showed that µPADs of group A stored at room temperature had good stability for up to 2 days, while µPADs of group B stored in a refrigerator showed acceptable performance for up to 6 days. This storage time is within the acceptable and moderate range compared to some reports. For example, Jayawardane et al. reported only 1 day of stability at room temperature [28]. In contrast, Ferreira et al., who designed a µPAD to measure these ions in human saliva, reported 14 days of stability for nitrate and 60 days for nitrite under ideal conditions, including storage in a vacuum at 4 °C, while under normal conditions, the stability of the device decreased significantly. Overall, although the µPAD storage time presented in this study is shorter compared to some complex methods that require special conditions, it offers an acceptable performance in terms of stability for short-term field applications, because of its simple construction, lack of need for special equipment, and easy usability.

4. Conclusion

In this study, a low-cost, disposable µPAD was developed for the colorimetric measurement of nitrite and nitrate in water. Nitrite was measured by the Griess reaction, while nitrate was measured after being reduced by ZnNPs. Nitrate was reduced to nitrite more effectively by ZnNPs than by ZnMPs. The system showed a linear range of 0.01 – 1.25 mM for nitrite and 0.04 – 1.25 mM for nitrate under optimal conditions, with detection limits of 0.003 and 0.008 mM, respectively. No significant interference from. Common ions was observed, and the results of real samples were consistent with the spectrophotometric reference method. The method offers benefits such as simple fabrication, ease of use, low cost, portability, and rapid on-site screening capabilities. Key limitations are the need to improve the stability and shelf life of the reagents for long-term storage. In future work, the focus will be on stabilizing and standardizing smartphone-based reading.

Acknowledgement
We thank the Razi University Research Council and Iran National Science Foundation (INSF) for support of this work.

Authors Contribution
All authors have contributed equally to prepare the paper.

Availability of data and materials
The datasets generated during and/or analyzed during the current study are available from the corresponding author on reasonable request.

Conflict of interests
The authors declare that they have no known competing financial interests or personal relationships that could have appeared to influence the work reported in this paper.

References

[1] T. Segawa, S. Ishii, N. Ohte, A. Akiyoshi, A. Yamada, F. Maruyama, Z. Li, Y. Hongoh, and N. Takeuchi. The nitrogen cycle in cryoconites: naturally occurring nitrification-denitrification granules on a glacier. *Environ. Microbiol*, **16**(10):3250–3262, (2014).

[2] A. Kurunc, S. Ersahin, B. Y. Uz, N. K. Sonmez, I. Uz, H. Kaman, G. E. Bacalan, and Y. Emekli. Identification of nitrate leaching hot spots in a large area with contrasting soil texture and management. . *Agric. Water Manag.*, **98**(6):1013–1019, (2011).

[3] A. Ahluwalia, M. Gladwin, G. D. Coleman, N. Hord, G. Howard, D. B. Kim-Shapiro, M. Lajous, F. J. Larsen, D. J. Lefer, L. A. McClure, and B. T. Nolan. Dietary nitrate and the epidemiology of cardiovascular disease: report from a National Heart, Lung, and Blood Institute Workshop. *J. Am. Heart Assoc.*, **5**(7):e003402, (2016).

[4] J. J. Sindelar and A. L. Milkowski. Human safety controversies surrounding nitrate and nitrite in the diet. . *Nitric oxide*, **26**(4): 259–266, (2012).

[5] S. F. Johnson. Methemoglobinemia: Infants at risk. . *Curr. Prob. Pediatr ad.*, **49**(3):57–67, (2019).

[6] N. S. Bryan and H. Van Grinsven. The role of nitrate in human health. . *Adv. Agron.*, **119**:153–182, (2013).

[7] P. I. Reed, K. Haines, P. L. Smith, F. R. House, and C. L. Walters. Gastric juice N-nitrosamines in health and gastroduodenal disease. *Lancet*, **318**(8246):550–552, (1981).

[8] H. R. Ghaffari, M. Yunesian, R. Nabizadeh, S. Nasseri, A. Sadjadi, F. Pourfarzi, H. Poustchi, and A. Eshraghian. Environmental etiology of gastric cancer in Iran: a systematic review focusing on drinking water, soil, food, radiation, and geographical conditions. . *Environ. Sci. Pollut. Res.*, **26**(11):10487–10495, (2019).

[9] G. Liu, H. Guo, W. Zhao, H. Yan, E. Zhang, and L. Gao. Advancements in preprocessing and analysis of nitrite and nitrate since 2010 in biological samples: a review. *Molecules*, **28**(20):7122, (2023).

[10] Q. Wang, L. J. Yu, Y. Liu, L. Lin, R. G. Lu, J. P. Zhu, L. He, and Z. L. Lu. Methods for the detection and determination of nitrite and nitrate, A review. *Talanta*, **165**:709–720.

[11] E. Wierzbicka. Novel methods of nitrate and nitrite determination, a review. *J. Elem.*, **25**(1):96–107, (2020).

[12] T. Fang, H. Li, G. Bo, K. Lin, D. Yuan, and J. Ma. On-site detection of nitrate plus nitrite in natural water samples using smartphone-based detection. *Microchemical Journal*, **165**:106117, (2021).

[13] A. M. López-Marzo and A. Merkoçi. Based sensors and assays, a success of the engineering design and the convergence of knowledge areas. . *Lab. Chip.*, **16**(17):3150–3176, (2016).

[14] E. W. Nery and L. T. Kubota. Sensing approaches on paper-based devices, a review. *Anal. Bioanal. Chem.*, **405**(24):7573–7595, (2013).

[15] E. Trofimchuk, Y. Hu, A. Nilghaz, M. Z. Hua, S. Sun, and X. Lu. Development of paper-based microfluidic device for the determination of nitrite in meat. *Food Chem.*, **316**:126396, (2020).

[16] M. Chaharlangi, J. Tashkhourian, M. M. Bordbar, R. Brendel, P. Weller, and B. Hemmateenejad. Apaper-based colorimetric sensor array for discrimination of monofloral European honeys based on gold nanoparticles and chemometrics data analysis. *Spectrichim. Acta. A.*, (2020).
DOI: https://doi.org/10.1016/j.saa. 2020.119076.

[17] S. Das, Gagandeep, and R. Bhatia. Based microfluidic devices: Fabrication, detection, and significant applications in various fields. *Reviews in Analytical Chemistry*, **41**(1):112–36.9, (2022).

[18] Anushka, A. Bandopadhyay, and Das P. K. Paper based microfluidic devices: a review of fabrication techniques and applications. . *The European Physical Journal Special Topics*, **232**(6):781–815, (2023).

[19] D. M. Cate, J. A. Adkins, J. Mettakoonpitak, and C. S. Henry. Recent developments in paper-based microfluidic devices. . *Anal. Chem.*, **87** (1):19–41.

[20] C. Dincer, R. Bruch, E. Costa-Rama, M. T. Fernández-Abedul, A. Merkoçi, A. Manz, G. A. Urban, and F. Güder. Disposable sensors in diagnostics, food, and environmental monitoring. *Adv. Mater.*, **31**(30):1806739, (2019).

[21] W. Li, X. Ma, Y. C. Yong, G. Liu, and Z. Yang. Review of paper-based microfluidic analytical devices for in-field testing of pathogens. . *Analytica Chimica Acta.*, **1278**:341614, (2023).

[22] Z. Yao, P. Coatsworth, X. Shi, J. Zhi, L. Hu, R. Yan, F. Güder, and H. D. Yu. Based sensors for diagnostics, human activity monitoring, food safety and environmental detection. *Sensors & Diagnostics.*, **1** (3):312–42, (2022).

[23] Y. Xia, J. Si, and Z. Li. Fabrication techniques for microfluidic paper-based analytical devices and their applications for biological testing: A review. *Biosens. Bioelectron.*

[24] F. T. Ferreira, R. B. Mesquita, and A. O. Rangel. Novel microfluidic paper-based analytical devices (μPADs) for the determination of nitrate and nitrite in human saliva. *Talanta*, **27**:121183, (2020).

[25] C. Y. Hou, L. M. Fu, W. J. Ju, and Wu P. Y. Microfluidic colorimetric system for nitrite detection in foods. . *Chem. Eng. J.*, **20**:125573, (2020).

[26] T. L. Mako, A. M. Levenson, and M. Levine. Ultrasensitive detection of nitrite through implementation of N-(1-naphthyl) ethylenediamine-grafted cellulose into a paper-based device. . *ACS Sens.*, **5**(4):1207–1215, (2020).

[27] F. Pena-Pereira, Ó. Matesanz, I. Lavilla, and C. Bendicho. A paper-based gas sensor for simultaneous noninstrumental colorimetric detection of nitrite and sulfide in waters. . *J. Sep. Sci.*, **43**(9-10): 1908–1914, (2020).

[28] B. M. Jayawardane, S. Wei, I. D. McKelvie, and S. D. Kolev. Microfluidic paper-based analytical device for the determination of nitrite and nitrate. *Anal. Chem.*, **86**(15):7274–7279, (2014).

[29] T. Tesfaye and A. Hussen. Microfluidic paper-based analytical device (μPAD) fabricated by wax screen printing technique for the determination of nitrite and nitrate ion in water samples. . *Microfluidics and Nanofluidics*, **26**(3):22, (2022).

[30] R. Catalan-Carrio, J. Saez, L. Á. Cuadrado, G. Arana, L. Basabe-Desmonts, and F. Benito-Lopez. Ionogel-based hybrid polymer-paper handheld platform for nitrite and nitrate determination in water samples. . *Analytica Chimica Acta.*, **1205**:339753, (2022).

[31] T. Thongkam and K. Hemavibool. An environmentally friendly microfluidic paper-based analytical device for simultaneous colorimetric detection of nitrite and nitrate in food products. . *Microchemical Journal*, **159**:105412, (2020).

[32] A. Charbaji, H. Heidari-Bafroui, N. Rahmani, C. Anagnostopoulos, and M. Faghri. Colorimetric determination of nitrate after reduction to nitrite in a paper-based dip strip. *Chemistry Proceedings*, **5**(1):9, (2021).

[33] L. Xie, X. Zi, H. Zeng, J. Sun, L. Xu, and S. Chen. Low-cost fabrication of a paper-based microfluidic using a folded pattern paper. . *Anal. Chim. Acta.*, **1053**:131–138, (2019).
DOI: https://doi.org/10.1016/j.aca.2018.12.001.

[34] C. K. Chiang, A. Kurniawan, C. Y. Kao, and M. J. Wang. Single step and mask-free 3D wax printing of microfluidic paper-based analytical devices for glucose and nitrite assays. *Talanta*, **194**:837–845, (2019).

[35] X Li, J. Tian, and W. Shen. Quantitative biomarker assay with microfluidic paper-based analytical devices. . *Anal. Bioanal Chem.*, **396**(1):495–501, (2010).

[36] P. Ghaderi-shekhi Abadi, F. H. Shirazi, M. Joshaghani, and H. R. Moghimi. Influence of formulation of ZnO nano-blokes containing metallic ions dopants on their cytotoxicity and protective factors: An in vitro study on human skin cells exposed to UVA radiation. *Toxicol. Rep.*, **5**:468–479, (2018).

[37] A. C. Bratton and E. K. Marshall. Synthesis and comparative study of the structural and optical properties of binary ZnO-based composites for environmental applications. *J. Biolog. Chem.*, **128**(2):537–550, (1939).